Asynchronous Suppression of Superficial Cortex during Absence Seizures

Meyer JFH*, Maheshwari A*, Noebels JL*, and Smirnakis SM†

*Department of Neurology, Baylor College of Medicine; †Harvard Medical School

Introduction

The *stargazer* mouse model of absence epilepsy has frequent, recurrent spike-wave seizures associated with behavioral arrest[1]. The mutation in *stargazer* mice leads to mistrafficking of AMPA receptors in fast-spiking interneurons in the neocortex which has been linked to interneuron-dependent paradoxical seizure exacerbation in the setting of NMDA receptor blockade[2]. However, the effect of this trafficking defect on cellular activity and network synchrony in the cortex has not been explored. In vivo two-photon microscopy permits the visualization and analysis of dozens of neurons simultaneously[4], and with concurrent EEG recordings, we examined the temporal dynamics of neuron and neuropil activity profiles during and around seizures.

Methods

AAV 2.1 GCamp6M virus is injected (100 nL) in V1 of 6 week old stargazer mice. 1 mm long, flat Ag/Ag-Cl electrodes are placed epidurally over ipsilateral somatosensory cortex and contralateral V1, and a titanium headpost is then permanently attached with dental cement. After 4 weeks, there is sufficient expression (left: z-stack max projection). A 3 mm cranial window is then placed over the injected area.

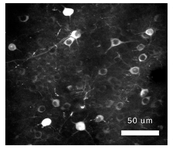

The EEG signal is sampled at 2 kHz with cut-offs at 1 Hz and 250 Hz. Seizures are detected manually using the following criteria: 6-10 Hz frequency, amplitude 2.5x above the baseline, and spike and wave morphology.

Raw calcium traces are acquired on a Prairie Ultima IV 2-photon microscope at 890 nm using spiral galvo scanning (14 – 20 Hz frame rate). They are converted into estimated firing rate using a filtering algorithm that estimates firing rate accurately[5]. Further analysis of calcium activity with respect to seizure onset/offset are performed in Matlab, with statistical analysis done in Graphpad Prism 7.

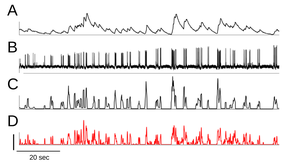

A patched, Gcamp6-filled neuron showing a DF/F trace **(A)**, the corresponding spike trace **(B)**, the extrapolated firing rate **(C)**, and the deconvolved firing rate **(D)**. (vertical scale bar: 100% DF/F (in A) or 10 Hz (in C, D)).

Superficial neurons and neuropil can be classified as 'ictal low', 'ictal high', or 'neutral'

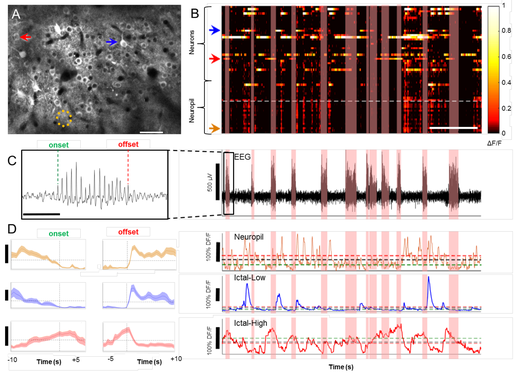

(A) Typical field of view for in vivo imaging; red – high activity during seizures (ictal-high neuron); blue – low activity during seizures (ictal-low neuron); orange dotted circle = neuropil patch. Bar = 50µm. **(B)** (top) Calcium activity for each neuron and neuropil patch over time with seizure epochs highlighted in pink (horizontal bar = 1 minute), with concomitant EEG and traces of calcium activity from the depicted neuropil, ictal-low neuron, and ictal-high neuron from A. Mean ictal activity (green dashed line), mean interictal activity (red dashed line), and overall mean activity (black dashed line) are plotted. Inset **(C)** shows definition of seizure onset and offset at first and last spike of the seizure, respectively (bar = 1 second). **(D)** Average activity (mean±SEM, vertical bar = 20% ΔF/F) of an exemplary neuropil patch (top), ictal-low neuron (middle), and ictal-high neuron (bottom) are shown, time locked to the seizure onset (left) and offset (right).

The majority of superficial neurons and neuropil patches have reduced activity during seizures

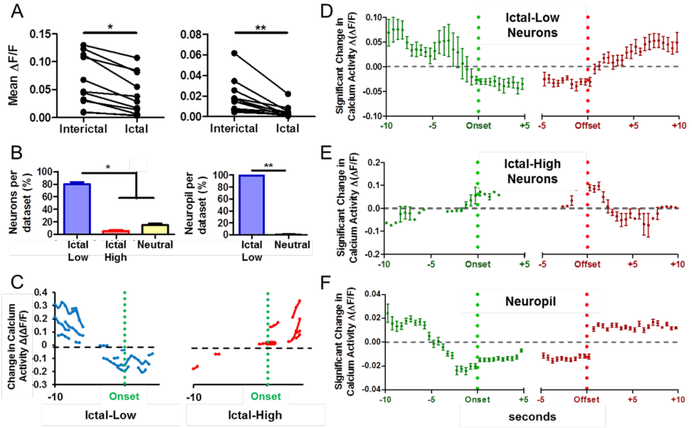

(A) Average calcium activity (ΔF/F) was significantly reduced in the ictal state compared to the interictal state for both neurons (left, *p<0.0005) and neuropil (right, *p<0.0025, n=11). **(B)** Significantly greater percentage of ictal-low neurons per dataset than ictal-high or neutral (left, *p<0.001); and significantly greater ictal-low neuropil patches compared to neutral (right, **p<0.001). **(C)** Example of intermittent participation of all ictal low (blue, left) and ictal high (red, right) neurons relative to seizure onset from two datasets. Temporal profile of significant change in **(D)** ictal-low neuron activity compared to baseline (n/bin=6-65 neurons); **(E)** ictal-high neurons (n/bin=0-5 neurons); and **(F)** neuropil activity (n/bin=9-61 neurons).

With chronic recordings, seizure participation of neurons varies over minutes to days

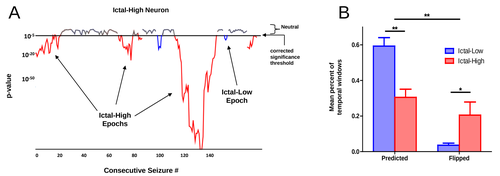

(A) With a 7-minute moving window, a neuron with an overall classification of "ictal-high" has 4 significant ictal-high segments (red), but also flips to have 2 ictal-low epochs (blue)
(B) Temporal windows were more often in the predicted than the flipped classification. In addition, ictal-low neurons had a smaller proportion of flipped classification than ictal-high neurons.

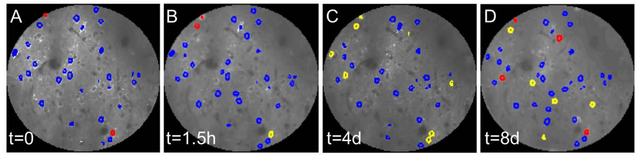

(A) Distribution of ictal-high and ictal-low neurons in one dataset, **(B)** 90 minutes later, **(C)** after 4 days, and **(D)** after 8 days in the same chronically imaged window. Blue=Ictal-low, Red=Ictal-High, Yellow=Neutral.

Patch-clamp recordings in a subset of animals confirm predominant ictal-low character of L2/3 neurons.

Mean±SEM ictal and interictal firing rates calculated from action potentials. 8 of 9 cells were deemed ictal low **(A)**, whereas 1 cell was ictal high **(B)**; *p<0.005, Mann-Whitney U test.

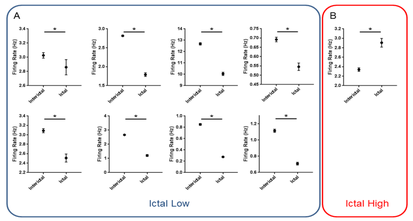

Asynchronous suppression of Layer 4 neurons.

(A) In 3 mice, Layer 4 neurons and neuropil showed significantly reduced activity (*p<0.05, Wilcoxon matched-pairs signed rank test); **(B)** Similar to L2/3, L4 neurons and neuropil also showed significantly reduced pairwise correlation (median with interquartile range, *p<0.0001, Wilcoxon matched-pairs signed rank test).

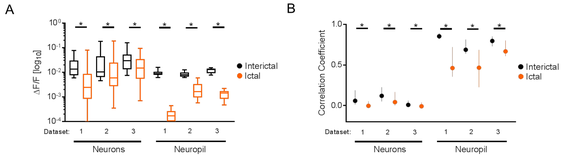

Pairwise synchrony is reduced in the ictal state

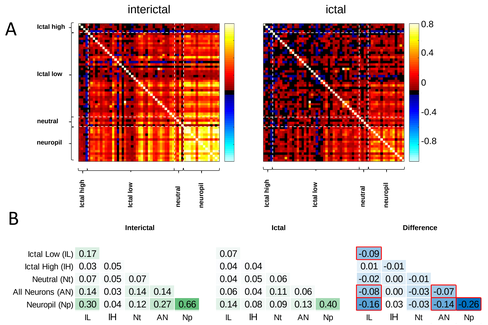

(A) Example of correlation coefficients in the interictal and ictal state in one recording. Matrix rows and columns are sorted into ictal high, ictal low, neutral and neuropil ROIs. **(B)** Baseline interictal correlations (left) were positive for all populations, most notably in the neuropil (Np). Correlations remained overall positive in the ictal state (middle). Correlation strength is represented in a green color scale. Note that correlation strength dropped in the ictal state. The ictal minus interictal difference in correlation strength (blue color scale) is shown on the right table, labeled "Difference." A red border outlining a value indicates that it reached significance (p<0.05). IL= Ictal Low; Nt = Neutral; AN = All Neurons; Np = Neuropil. Of note, in 2 separate datasets with all locomotion frames removed, both activity and pairwise correlation of neurons and neuropil remained significantly reduced in the ictal state (data not shown). **(C)** Synchrony was reduced in the ictal state relative to the interictal state for all neuron, neuropil and ictal-low pairwise comparisons (Int = interictal; Ict = Ictal); n=11 datasets from n=9 animals, *p=0.014, **p<0.005).

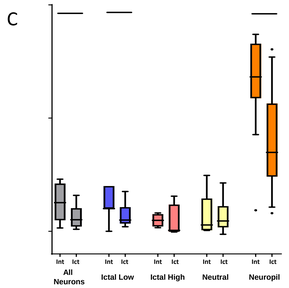

References

1. Noebels, J. L., Qiao, X., Bronson, R. T., Spencer, C. & Davisson, M. T. Stargazer: a new neurological mutant on chromosome 15 in the mouse with prolonged cortical seizures. *Epilepsy Res.* **7,** 129–135 (1990).
2. Maheshwari, A., Nahm, W. K. & Noebels, J. L. Paradoxical proepileptic response to NMDA receptor blockade linked to cortical interneuron defect in stargazer mice. *Front Cell Neurosci* **7,** 156 (2013).
3. Sippy, T. & Yuste, R. Decorrelating action of inhibition in neocortical networks. *J. Neurosci.* **33,** 9813–9830 (2013).
4. Chen, T.-W. *et al.* Ultrasensitive fluorescent proteins for imaging neuronal activity. *Nature* **499,** 295–300 (2013).
5. Vogelstein, J.-T. et al., Fast nonnegative deconvolution for spike train inference from population calcium imaging. J Neurophysiol. **104(6)**, 3691-3704, 2010

Sources of funding

J Meyer/S Smirnakis: NIH R21 NS088457; A Maheshwari: NIH K08 NS096029-01; J Noebels: NIH R01 29709